BRL

REPORT NO. 1650

EFFECTS OF A MAGNETIC FIELD ON BURNING RATE OF SOLID PROPELLANT

by

Webster M. Kendrick
Leland A. Watermeier
William P. Aungst
Samuel P. Pfaff

June 1973

USA BALLISTIC RESEARCH LABORATORIES
ABERDEEN PROVING GROUND, MARYLAND

BALLISTIC RESEARCH LABORATORIES

REPORT NO. 1650

JUNE 1973

EFFECTS OF A MAGNETIC FIELD ON BURNING RATE OF SOLID PROPELLANT

Webster M. Kendrick
Leland A. Watermeier
William P. Aungst
Samuel P. Pfaff

Interior Ballistics Laboratory

RDT&E Project No. 1T161102A33C

ABERDEEN PROVING GROUND, MARYLAND

B A L L I S T I C R E S E A R C H L A B O R A T O R I E S

REPORT NO. 1650

WMKendrick/LAWatermeier/WPAunqst
SPPfaff/mfp
Aberdeen Proving Ground, Md.
June 1973

EFFECTS OF A MAGNETIC FIELD ON BURNING RATE OF SOLID PROPELLANT

ABSTRACT

Preliminary experiments conducted by the Interior Ballistics Laboratory to determine if a magnetic field applied during low pressure combustion of solid propellant can alter the burning rate have shown positive results. Experiments were conducted with a field strength of 15000 gauss applied to composite propellants containing aluminum additive burning at atmospheric and sub-atmospheric pressures. Although results showed wide scatter of data, it appears that burning rate variations of ± 10% could be obtained.

TABLE OF CONTENTS

LIST OF ILLUSTRATIONS

SPECIAL NOTE

The following report represents some work that was done several years ago in BRL. For various reasons, a draft report only was written, reviewed with the coauthors, and subsequently set aside. Following the untimely death of the principal author, Mr. Webster M. Kendrick, in 1971, the draft copy of this report was found in his personal effects. It is conjectured that although the experiments were run some time ago, the data, theory and procedures may still be of interest and value to the scientific community concerned with propellant combustion technology. Hence, its publication at this late date.

I. INTRODUCTION

Experiments have been conducted in the Interior Ballistics Laboratory to determine if a magnetic field applied during the low pressure combustion of solid propellant can alter the burning rate.

Various investigators have reported ion concentrations up to 10^{12} per cc in ordinary gaseous flames,[*1] and experiments have shown that the gaseous products of solid propellant burning are weakly ionized, i.e., ion densities are much less than 10^{-6} of the total particle densities. In many cases, however, the reaction zone extends only 100 microns or less from the burning surface, and the accuracy of current estimates of ion density in this zone is doubtful. If ions play a significant part in the combustion process and if their concentration is greater than ordinary methods of observation suggest, these facts should be confirmed by applying a sufficiently strong magnetic field to the burning propellant. An experiment has been conducted to detect any substantial influence of a magnetic field on the burning rate of composite propellants and to explore the possibility of control of the burning rate after ignition. First indications were that there was a detectable influence.

II. THEORY OF AMBIPOLAR DIFFUSION IN MAGNETIC FIELD

The following discussion was derived by the principal author (W.M.K.), who relied heavily on Reference 2.

A realistic plasma has two types of charged particles, electrons and ions, and will have almost precise charge neutrality except in a thin sheath region close to a material wall. The requirement of near-neutrality is easily shown. Suppose that the electron density in a plasma is denoted by n and that the ions are entirely absent over a thin, slab-like region of the plasma of half-thickness x. The resultant potential difference from the center to the outside of the slab region

* References are listed on page 32

is readily calculated

$$\frac{\partial^2 V}{\partial x^2} = 4\pi ne \tag{1}$$

and

$$\Delta V = 2\pi ne \cdot x^2. \tag{2}$$

The change in potential energy of an electron across this slab is then

$$\Delta E = 2\pi ne^2 x^2. \tag{3}$$

It is convenient to define a characteristic length in a plasma, denoted by h, which is the value of x for which the change in potential energy equals the mean kinetic energy, $\frac{1}{2}kT$, in one direction. Thus

$$h = \sqrt{\frac{kT}{4\pi ne^2}}. \tag{4}$$

This quantity, h, is called the "Debye shielding length" since it is clearly a measure of the distance over which the electron charge density can differ appreciably from the ion charge density. For example, over a region whose thickness is ten times h, the electron charge density must equal the ion charge density within 1% if the electrical potential energy is not to exceed the mean kinetic energy. Of course, the electrical potential energy cannot be larger than the mean thermal energy since the charged particles will then move so as to restore neutrality.

It is assumed that h is small compared to other lengths of interest in the plasma. In fact, this is the definition of a plasma. If kT is in electron volts, equation (4) may be rewritten as

$$h = 740\sqrt{\frac{kT}{n}} \tag{5}$$

A typical arc plasma may have an electron density of about 10^{12} and a temperature in the neighborhood of an electron volt or so. Hence, the Debye shielding length is less than 10^{-3} cm. It should be noted that the Debye shielding length is a measure of the thickness of the sheath region which develops wherever the plasma is in contact with a solid surface.

A weakly-ionized plasma will be defined as a plasma in which the mean free path for electron-neutral atom collisions and for ion-neutral atom collisions is small compared to the mean free path for appreciable deflections by coulomb collisions between the charged particles. A plasma of this type is particularly susceptible to analysis since the charged-particle conservation conditions will be linear in the particle densities. As a result, the intrinsic diffusion coefficient for electrons in the absence of a magnetic field is

$$D_o^- = \frac{\lambda^- v^-}{3} \tag{6}$$

and that of the ions is

$$D_o^+ = \frac{\lambda^+ v^+}{3}, \tag{7}$$

where λ is the mean free path for collisions with a neutral target and v is the charged-particle velocity. The superscripts - and + denote electrons and ions, respectively. In general, the mean free paths will be comparable, while the electron velocity will be very much larger than that of the ion at comparable temperatures. Since the electron-density gradient must be the same as the ion-density gradient, owing to the requirement of space charge neutrality, it is clear that the electrons would tend to stream out of the plasma much more rapidly than the ions.

A situation of this sort is incompatible with the requirement of plasma neutrality and hence electric fields will immediately develop so as to retard the electrons and produce equal streaming losses of electrons and ions from the plasma. The resultant diffusion rate may be calculated by including the added "mobility" of a charged particle due to an applied electric field.

Once again, a one-dimensional argument will be used. Consider a particle which has suffered a collision at the point which is a distance s to the left of a unit area dA located at the origin of Figure 1. Assume that the particle acquires the average thermal velocity v, as a result of this collision, with equal probability to the left and right. It subsequently is accelerated to the right at

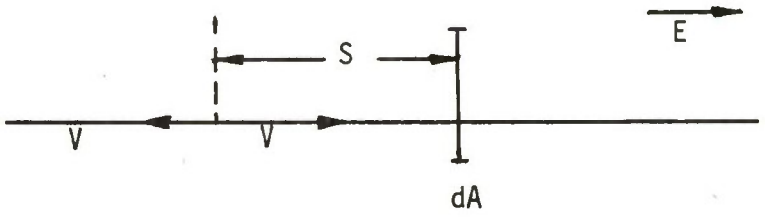

Figure 1. Mobility of a Charged Particle

the constant rate eE/m. It is assumed that the net increment of velocity between collisions is small compared to the thermal velocity. As a result, those particles moving to the left after the collision will not pass through dA, while those moving to the right reach dA with an increased velocity v' given by

$$v' = \sqrt{(v^2 + 2as)} \tag{8}$$

where a = eE/m is the acceleration.
Hence the flux through dA from the left is

$$F_L = \int_0^\infty \frac{n}{2\lambda} - (v^2 + 2as)\exp(-s/\lambda)ds. \tag{9}$$

Note that n/2 is used rather than n/6. The reason for this is the fact that particles moving in all three dimensions are accelerated to the right by the electric field. The desired result may be obtained by expanding the square root term in powers of as/v and subtracting the flux from the right. The first non-vanishing term is

$$F = \frac{na\lambda}{v} \int_0^\infty \frac{s}{\lambda} \exp(-s/\lambda) \frac{ds}{\lambda} \tag{10}$$

$$= \frac{na\lambda}{v} = \frac{e\lambda}{mv} nE. \tag{11}$$

The mobility, μ, is defined to be the coefficient of nE in the expression for the flux. (Note that its sign depends on the charge.) Hence

$$F = n\mu E \tag{12}$$

and

$$\mu = \frac{e\lambda}{mv}. \tag{13}$$

Rewriting this,

$$\mu = \lambda v \cdot \frac{e}{mv^2} \frac{e}{kT} = \frac{eD}{kT}, \tag{14}$$

where D is the usual diffusion coefficient.

An expression may now be obtained for the common rate of streaming of electrons and ions out of the plasma. The electron flux has the form

$$\bar{F} = - D_o \frac{\bar{\partial n}}{\partial x} + \bar{n} \bar{\mu}_o \bar{E}_x, \tag{15}$$

with a similar expression for the ions. Both the density gradient and the electric field are assumed to exist in the x-direction only. The resultant particle conservation equation is

$$\frac{\partial n^-}{\partial t} = -\nabla \cdot F^- = -\frac{\partial F^-}{\partial x} \tag{16}$$

$$\therefore \frac{\partial n^-}{\partial t} = D_o^- \frac{\partial^2 n^-}{\partial x^2} - \mu_o^- \frac{\partial}{\partial x}\left[n^- E_x\right], \tag{17}$$

while the corresponding expression for the ions is

$$\frac{\partial n^+}{\partial t} = D_o^+ \frac{\partial^2 n^+}{\partial x^2} - \mu_o^+ \frac{\partial}{\partial x}\left[n^+ E_x\right] . \tag{18}$$

By the basic assumption of near neutrality of the plasma, $n^+ = n^- = n$. Thus the electric field term may be eliminated by multiplying equation (17) by μ_o^+, equation (18) by μ_o^-, and subtracting. The result is

$$\frac{\partial n}{\partial t} = \frac{\mu_o^+ D_o^- - \mu_o^- D_o^+}{\mu_o^+ - \mu_o^-} \frac{\partial^2 n}{\partial x^2} \tag{19}$$

It is clear that there is an effective diffusion coefficient common to both the electrons and ions. This "ambipolar" quantity is

$$D_o^{AMB} = \frac{\mu_o^+ D_o^- - \mu_o^- D_o^+}{\mu_o^+ - \mu_o^-} \tag{20}$$

Substitution from equation (14) yields an alternative form

$$D_o^{AMB} = \frac{D_o^+ D^- \left(1/kT_+\right) + \left(1/kT_-\right)}{\left(D_o^+/kT_+\right) + \left(D_o^-/kT_-\right)} \tag{21}$$

It was pointed out above that for comparable electron and ion temperatures, one has $D_o^- \gg D_o^+$. Hence equation (20)reduces in this case to

$$D_o^{AMB} \cong 2D_o^+ . \tag{22}$$

Equation (22) shows that the effective diffusion coefficient is approximately twice that of the slower component.

The situation when a magnetic field is present is apparently more complicated. However, it is not difficult to carry through a "curved one-dimensional" argument (Figure 2) just as in the case of the diffusion coefficient. The result is completely similar. The mobility μ across a magnetic field is

$$\mu = \frac{\mu_o}{1 + (\omega\tau)^2}, \tag{23}$$

where μ_o is the magnetic field-free result given in equation (13).

In most cases of experimental interest, the plasma density is sufficiently low and the field sufficiently large so that the quantities $(\omega\tau)^2$ for both electrons and ions are very much larger than unity. Since $\omega\tau = \lambda/r_o$ this means that the particles execute very many gyrations in the magnetic field before a collision occurs. It is clear that if the opposite situation is true, $(\omega\tau)^2 < 1$, the effect of the magnetic field is small and the field-free results of equations (6) to (22) will apply.

It can be shown that the effective diffusion coefficients are

$$D_{\perp}{}^{+} \cong \frac{D_o{}^{+}}{(\omega^{+}\tau^{+})^2} \tag{24}$$

$$D_{\perp}{}^{-} = \frac{D_o{}^{-}}{(\omega^{-}\tau^{-})^2}. \tag{25}$$

Note that these diffusion coefficients vary as the inverse square of the magnetic field strength and depend on the other variables, as follows

$$D \sim \frac{m^2 v^3}{\lambda B^2} = \frac{\sqrt{(m)(kT)^{3/2}}}{\lambda B^2}. \tag{26}$$

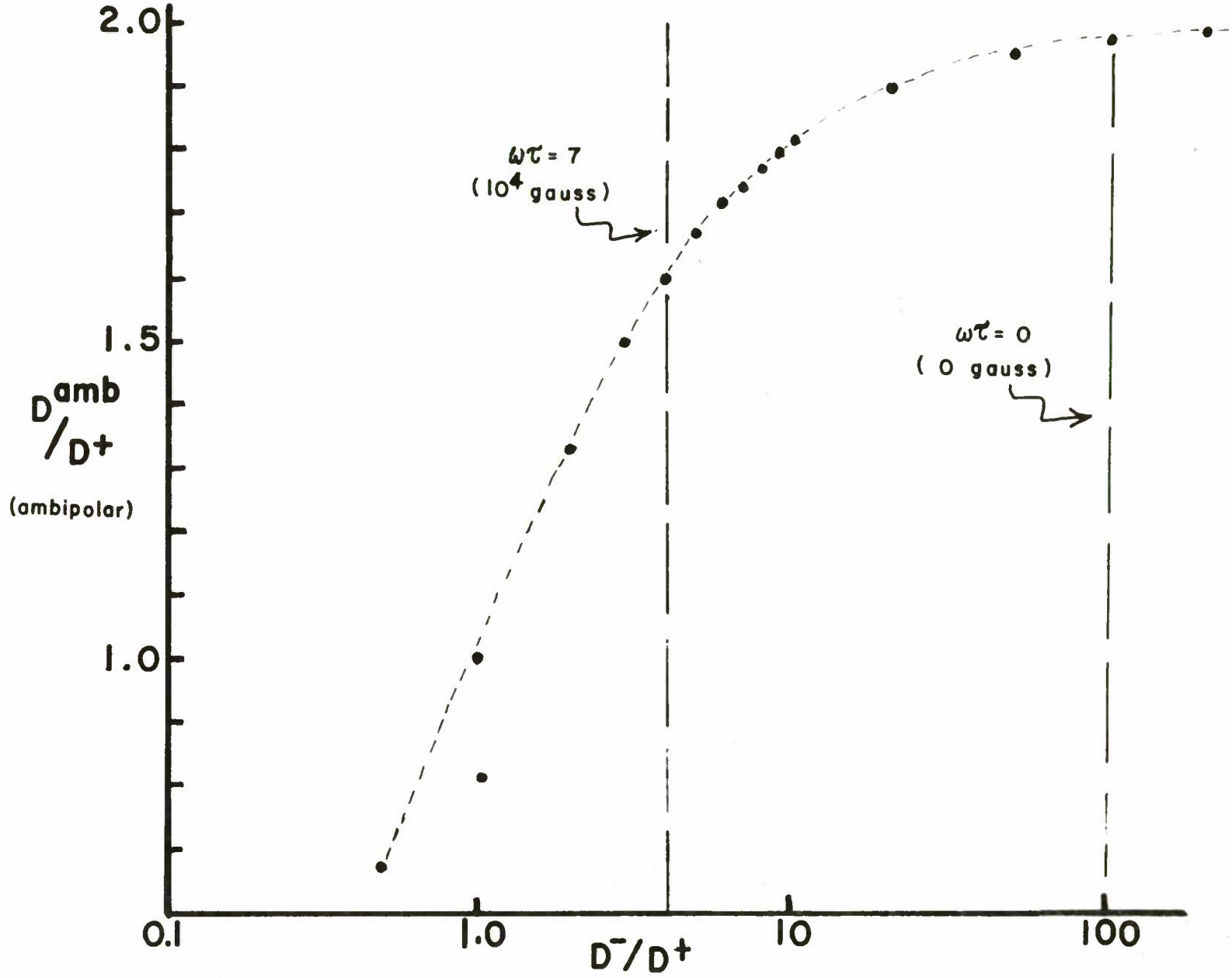

Figure 2. Curved one dimensional argument of ambipolar diffusion in a magnetic field.

Hence, for comparable temperatures and mean free paths, the ion diffusion coefficient is very much larger than that of the electrons. Thus

$$D_{\perp}^{+} \gg D_{\perp}^{-} . \tag{27}$$

The ions tend to diffuse across a magnetic field faster than the electrons, which is the reverse of the behavior in the direction of the field lines. Another way to see this is to recognize that diffusion across the field is by means of the random changes of the location of the center of the Larmor circle of the particle after each collision. This deflection is of the order of the Larmor radius. Hence the heavier particle diffuses faster since it has a larger Larmor radius. The same conclusions hold for the mobility of the particles.

Suppose that the magnetic field lines are infinitely long so that there is no diffusion of electrons or ions in this direction. In this hypothetical case, all diffusion is across the magnetic field, and once again an electric field must develop in this direction so as to equate the electron and ion fluxes and maintain charge neutrality. The argument given in equations (15) to (20) goes through exactly in this case, except that the subscript 0 is replaced by $\perp$ everywhere. Thus

$$D_{\perp}^{AMB} = \frac{\mu_{\perp}^{+} D_{\perp}^{-} - \mu_{\perp}^{-} D_{\perp}^{+}}{\mu_{\perp}^{+} - \mu_{\perp}^{-}}$$

$$= \frac{D^{+} D^{-} (1/kT_{+}) + (1/kT_{-})}{(D^{+}/kT_{+}) + D^{-} kT_{-})} \tag{28}$$

By use of equation (27),

$$D^{AMB} = 2D^{-} \tag{29}$$

for equal temperatures. Note that the "ambipolar" rate is again twice that of the slower component.

III. EXPERIMENTAL APPARATUS AND PROCEDURE

The basic components of the experimental apparatus are shown in the schematic Figure 3. Two coils were used, each of which consisted of 250 turns of a strip of copper .127mm thick x 50.8mm wide. The turns were interwound with an insulator of .0127mm thick Mylar plastic. The coils were mounted in an upright position approximately 31.75mm apart. They were connected in series through a fuse and high voltage switch to a 250 V.D.C. generator. When the entire generator output was used with the coils, a field strength of approximately 15,000 gauss resulted.

The combustion chamber was a 28.57mm O.D. glass tube placed upright between the coils. The bottom of the tube was closed with a plate through which nitrogen and the ignition leads were admitted. The upper end of the tube was closed off by a venting plate through which the gases could either be exhausted to the atmosphere or to a vacuum line.

Slabs of propellant (6.35mm x 19.05mm x 25.4mm) were used in these experiments. They were ignited on the top 6.35mm x 19.05mm edge by a hot wire igniter paste system. The slab then burned down in cigarette fashion. The sides were kept from burning by a nitrogen flow. When sub-atmospheric shots were made, the slab was ignited at one atmosphere and the pressure subsequently reduced to the desired level by the vacuum pump before starting the test.

The combustion process was recorded on 16mm film by a Fairchild Motion Analysis camera. The camera speed normally used was 1800 to 3000 frames per second. In an experimental run, the nitrogen flow was started and the propellant slab ignited. After three or four seconds of burning the camera was turned on and approximately four seconds of burning time was recorded before the magnetic field was turned on. After activation of the field, a fuse was blown in 0.3 to 3.0 seconds. The propellant continued to burn until the entire slab was consumed.

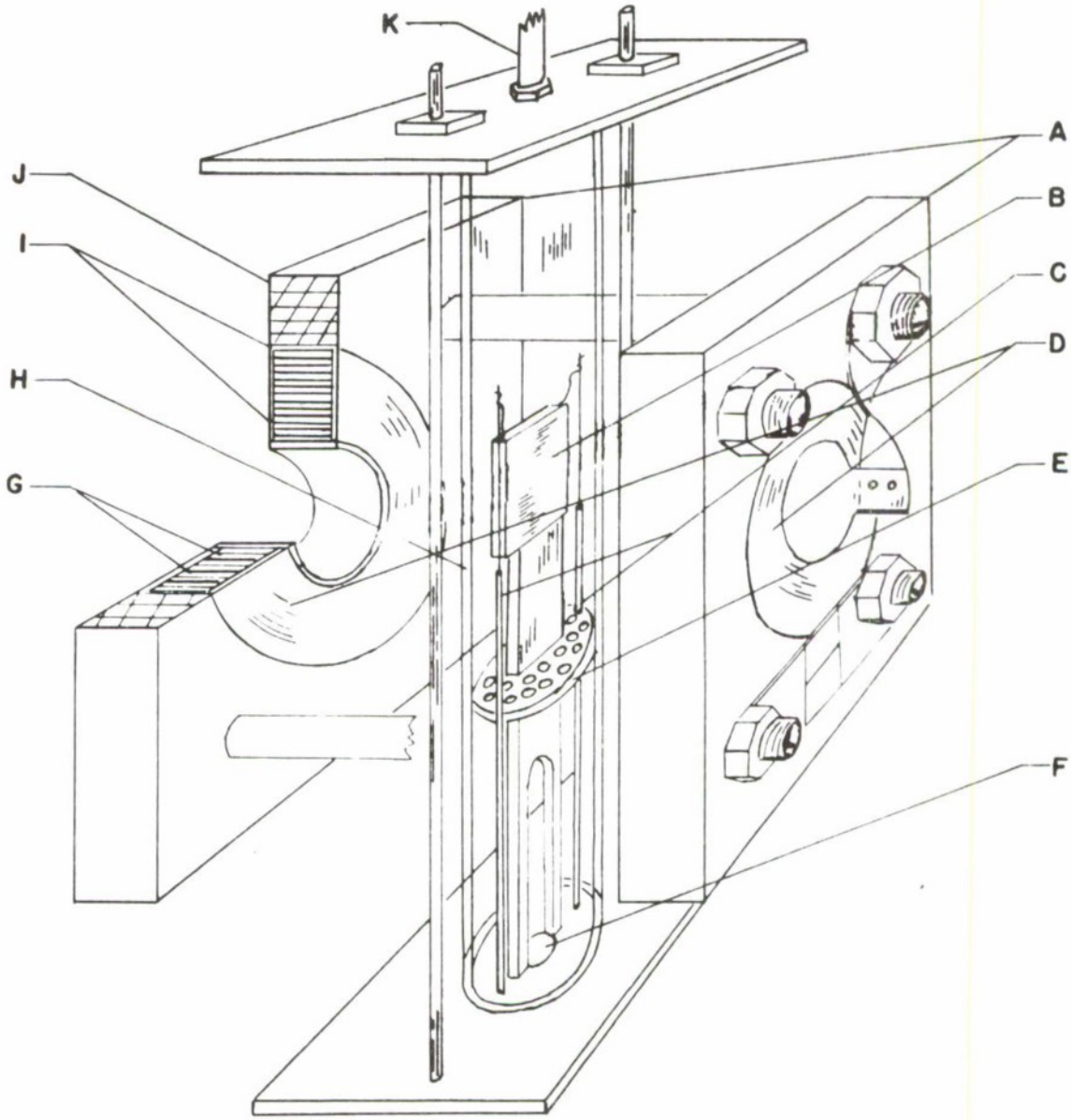

A— COIL HOUSING

B— PROPELLANT

C— IGNITION LEADS

D— COILS

E— DIFFUSION PLATE

F— NITROGEN SUPPLY INLET

G— COIL WINDINGS - MYLAR & COPPER

H— GLASS ENCLOSURE

I — POTTING COMPOUND

J— BAKELITE

K— EXHAUST

Figure 3. Schematic drawing (not to scale) of the experimental apparatus.

The total burning time recorded by the camera was about 8 seconds. In this way, many pictures were obtained of the burning propellant before, during, and after the introduction of the magnetic field. For sub-atmospheric runs, the camera was not turned on until the desired chamber pressure was attained.

Inked lines 4.74mm apart on the sides of the propellant slabs provided calibrated distance standards and were used in measuring the propellant regression rate as a function of time. These measurements were normally made at .05 second intervals determined by 100 cps timing marks on the film. The slopes of the least square straight line fits were then compared to determine the burning rate changes. The data points from the time before the magnetic field was turned on and after the field was turned off were combined for comparison with the time that the coils were energized. Figure 4 shows the raw data points and the least square fit lines for a typical run. To make the slope change more visible, the "before" and "after" data were not combined in this plot.

IV. EXPERIMENTAL RESULTS

Several runs were made trying different orientations of the field sense with respect to the burning surface. The results presented in Figure 5 are all cases in which a transverse field sense was used. Three types of propellant were fired: (1) a composite containing no metal additive and (2) two other composites which were basically of the same composition except one contained 2% (Thiokol DA-102) and the other contained 13% (Thiokol UR-101) by weight of powdered aluminum.

As can be seen, some burning rate variations were measured during the field operation. Only one run (at 1 atm. pressure) was made with the propellant containing no aluminum. It exhibited a 5% reduction in burning rate during the time the coils were activated. Successive frames from typical motion picture records of the aluminized propellants burning with and without magnetic field applied are shown in Figures 6, 7, 8, 9.

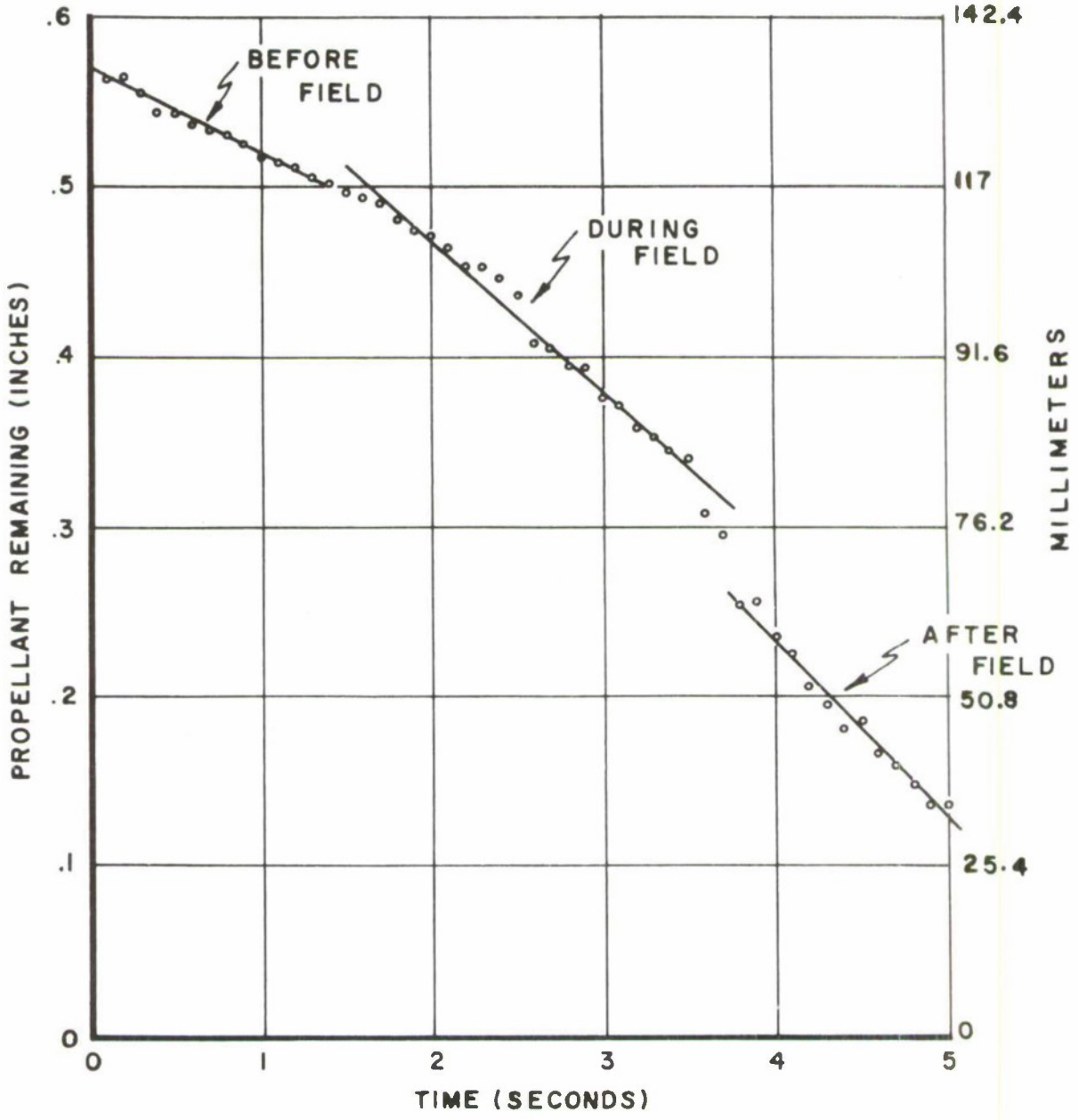

Figure 4. Plot of propellant regression rates during an experimental run at .66 atmosphere pressure. Propellant was a composite (Thiokol DA-102) containing 2% powdered aluminum.

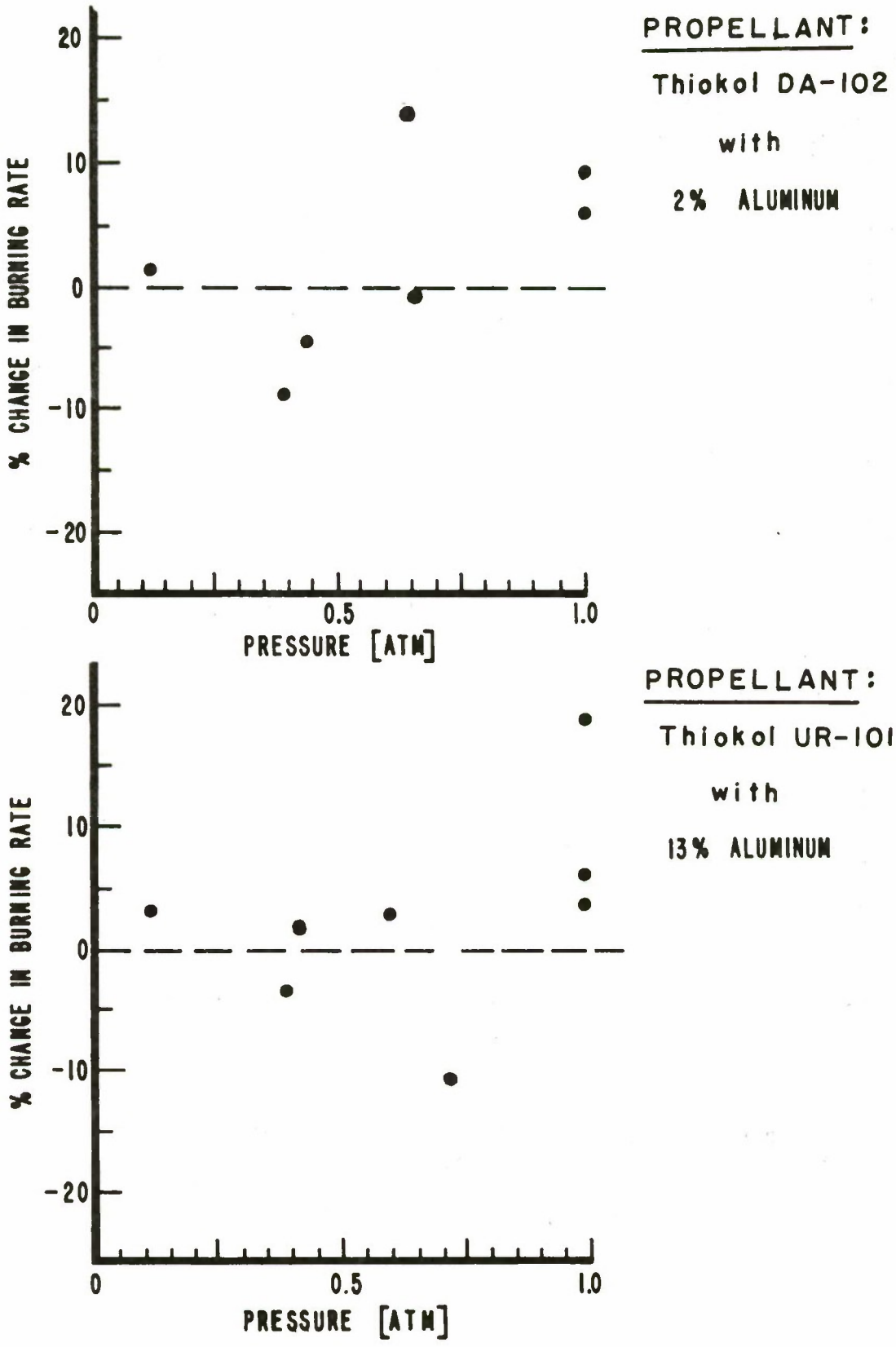

Figure 5. Graph showing experimentally determined variations from normal burning rates due to magnetic field effects.

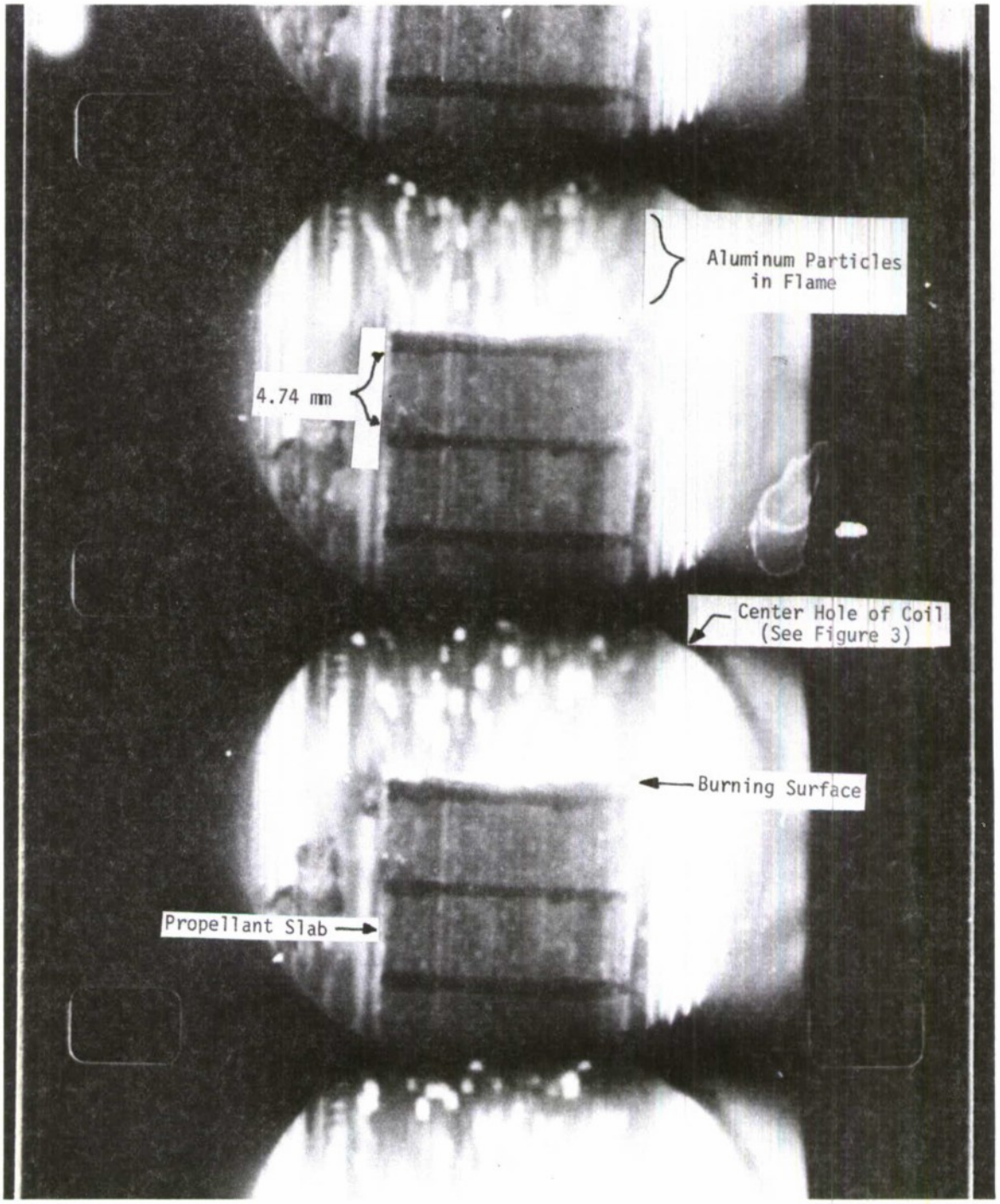

Figure 6. Successive frames (3000 fps) from motion pictures of propellant slab (THIOKOL UR-101) burning before magnetic field was applied.

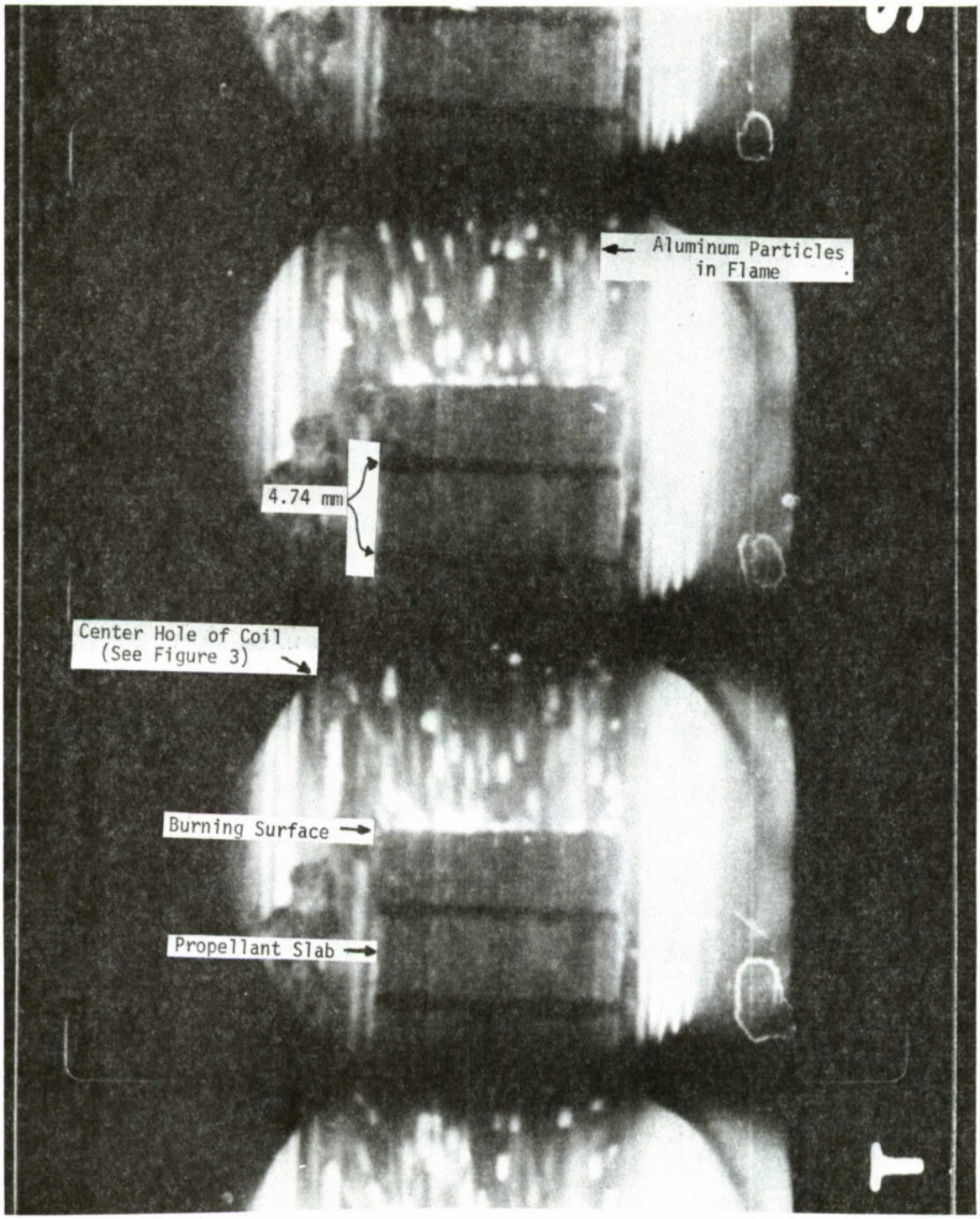

Figure 7. Successive frames (3000 fps) from motion pictures of propellant slab (THIOKOL UR-101) burning while magnetic field was applied. Note change in intensity of aluminum droplet burning.

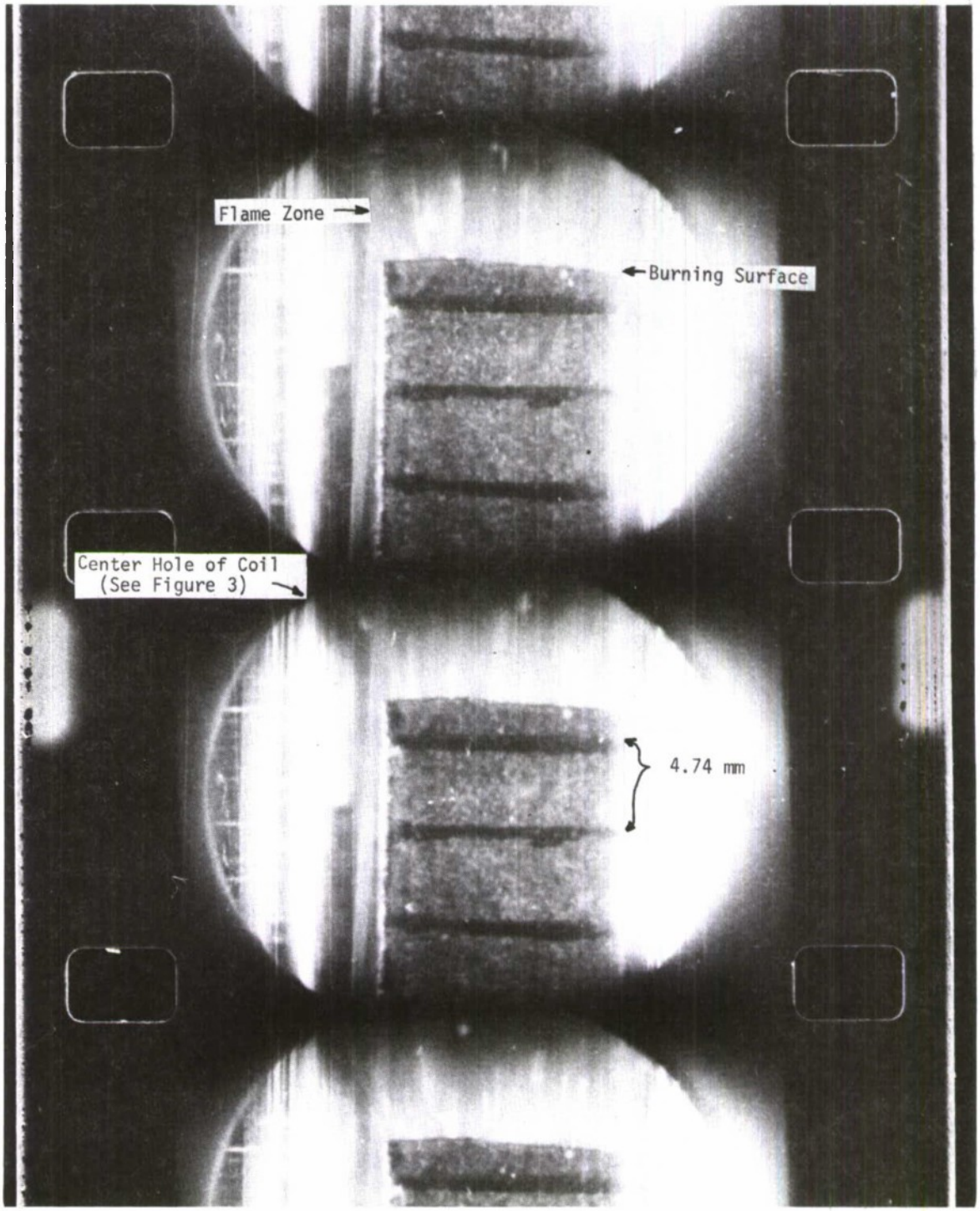

Figure 8. Successive frames (3000 fps) from motion pictures of propellant slab (THIOKOL DA-102) burning before magnetic field was applied.

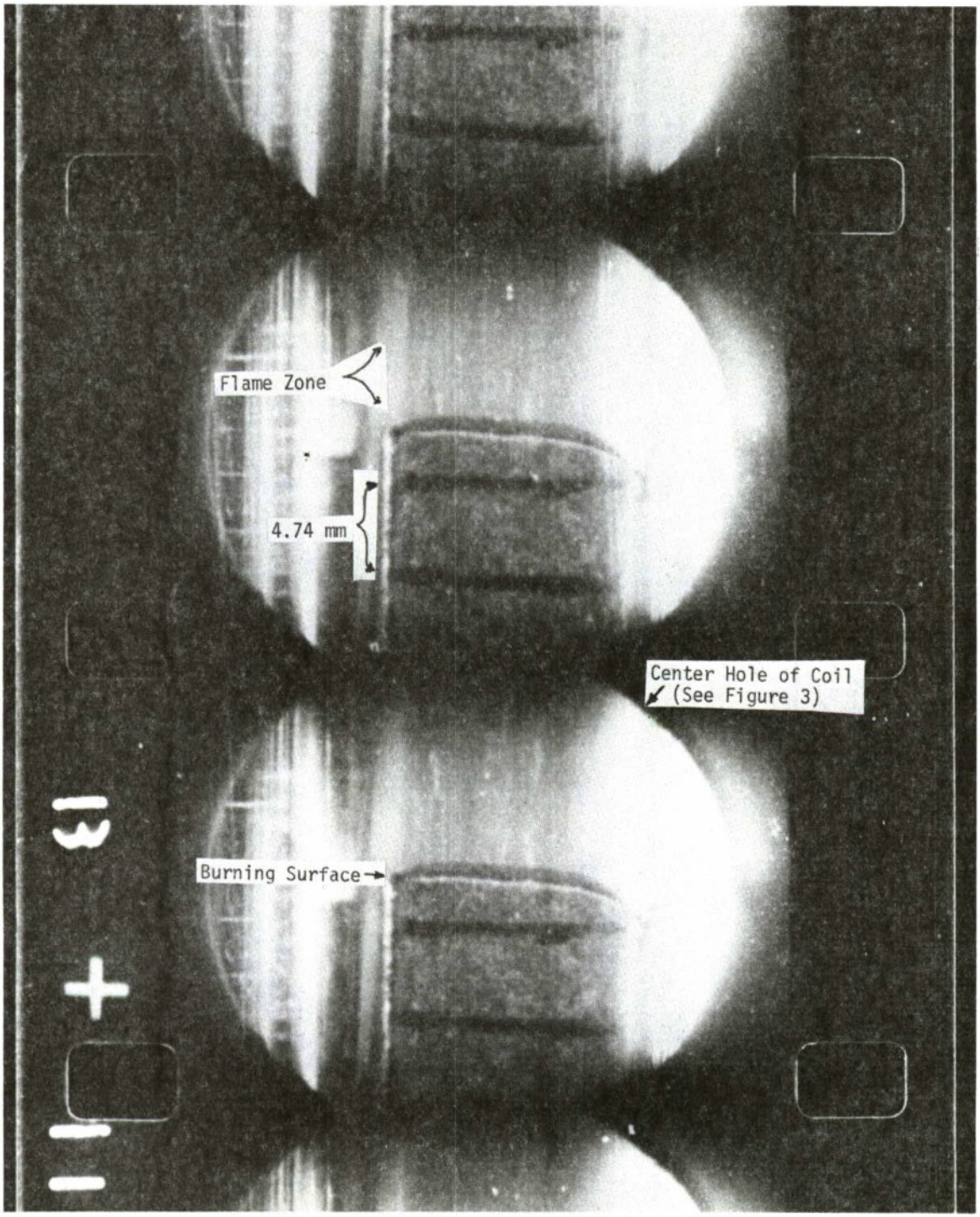

Figure 9. Successive frames (3000 fps) from motion pictures of propellant slab (THIOKOL DA-102) burning while magnetic field was applied. Note relative absence of burning aluminum droplets.

V. DISCUSSION

The following discussion of the diffusion coefficient in an ionized gas with the presence and absence of a magnetic field will illustrate possible contributions to the burning rate. Thermal conductivity in an ionized gas differs from diffusion in that ion-electron collisions are not of importance in thermal conductivity while they are significant in diffusion.

The equations governing diffusion are presented without derivation since this is available in standard texts. Nomenclature used follows that of Maxfield and Benedict.[2]

In these experiments, the flame temperature and the surface temperature are approximately 3000°K and 1000°K, respectively. It is assumed that 2000°K would be a close enough estimate to the temperature of the zone in which diffusion could have a controlling effect on the burning rate.

In a typical case, then: $p = 250\text{mm}$, $T = 2000°K$, $N = 10^{24}$ particles/meter^3, and $\sigma = 3\times10^{-10}$ meters, where σ is the diameter of a typical molecule.

The diffusion coefficient for charged particles moving transverse to a magnetic field is reduced from its zero field value as shown:

$$D = \frac{D_o}{1 + (\omega\tau)^2}$$

where D_o is the diffusion coefficient in the absence of a magnetic field, ω is the cyclotron frequency and τ is the mean time between collisions with neutral molecules. For electrons in a field of 15,000 gauss $\omega = 2.7\times10^{11}$ per second. Under the previously stated conditions, $\tau = 4.2\times10^{-11}$ seconds. The factor $\omega\tau$ becomes 11.3 and the diffusion rate of the electrons across the field has been reduced by a factor of approximately 130. This result is sensitive to the assumption about molecular cross section.

It might be thought that the field of 15,000 gauss would have little effect on positive ion diffusion since the decrease in ω with increased mass is more rapid than the increase in τ. The net decrease in $\omega\tau$ is proportional to the dquare root of the ratio of ionic to electronic mass. Indirectly, however, through the necessity for maintaining charge neutrality in the gas, the effect on positive ions is also significant. If the ionized region is insulated from any conduction path, the tendency of the electrons to rapidly diffuse out of the source region is countered by the electric field set up by the charge separation. The diffusion of electrons and ions out of the source region takes place at a common rate characterized by an expression known as the ambipolar diffusion coefficient. It is given by:

$$D^A = \frac{\mu^+ D^- - \mu^- D^+}{\mu^+ - \mu^-}$$

where μ is the mobility of the particles, and the + and - superscripts indicate ions and electrons, respectively. When D^- is much greater than D^+ the diffusion coefficient D^A_- is approximately equal to $2D^+$. In the absence of a magnetic field, $\frac{D^-}{D^+} = 220$ if the average molecular weight of the positive ions is taken as 25, while in a 15,000 gauss field the ratio is reduced to approximately 2.0 and the ambipolar diffusion coefficient is reduced accordingly. Under the given conditions, $D^A = 1.3D^+$. If the ionized component of the gas is only a small fraction of the total particles, this change of diffusion coefficient will contribute very little to the total diffusion, but if the ionized component is a large fraction then the results obtained in the magnetic field experiments can be considered reasonable. If combustion occurs essentially at the surface of the propellant, diffusion will cause a loss of energetic particles from the burning region. Application of a magnetic field will reduce this heat loss, thereby increasing the burning rate. If, on the other hand, the reaction occurs in a zone somewhat removed from the surface of the propellant, diffusion is required in order to allow energetic particles to reach the surface of the propellant and

produce a new source of reactive material. Application of a magnetic field in this case will cause a reduction in diffusion from the reactive zone to the propellant surface. This will decrease the amount of material evolved from the surface and thus lead to a reduction in burning rate. Either of these cases might be observed in practice, and there seems to be an indication from the experimental evidence that either can be observed, depending upon the pressure at which burning takes place.

ACKNOWLEDGMENTS

The assistance of Lawrence A. Peters (since retired) and Paul H. Sellers on problems related to development of the magnet coils is gratefully acknowledged.

Thiokol (Elkton Division) supplied the propellant samples used.

SPECIAL NOTE

Due to the untimely death of one author (W.M.K.), subsequent change of duties of another (L.A.W.) and reassignment of the other two authors (W.P.A. and S.P.P.), the work described in this report was not continued to attain the ultimate goals. It is hoped that the results will provide impetus to future efforts, however.

REFERENCES

1. See for example, Gaydon, A. G. and Wolfhard, H. G., "Flames: Their Structure, Radiation and Temperature" Chapter XIII, Chapman and Hall Ltd., London, 1953.

2. Maxfield, F. A. and Benedict, R. Ralph, "Theory of Gaseous Conduction and Electronics," Chapters IV, VII, and X, McGraw-Hill Book Company, Inc., New York, 1941.

DISTRIBUTION LIST

No. of Copies	Organization
12	Commander Defense Documentation Center ATTN: TIPCR Cameron Station Alexandria, Virginia 22314
1	Director Institute for Defense Analyses ATTN: Mr. H. Wolfhard 400 Army-Navy Drive Arlington, Virginia 22202
1	Commander U.S. Army Materiel Command ATTN: AMCDL 5001 Eisenhower Avenue Alexandria, Virginia 22304
1	Commander U.S. Army Materiel Command ATTN: AMCDMA, MG J.R.Guthrie 5001 Eisenhower Avenue Alexandria, Virginia 22304
1	Commander U.S. Army Materiel Command ATTN: AMCRD, MG S. C. Meyer 5001 Eisenhower Avenue Alexandria, Virginia 22304
1	Commander U.S. Army Materiel Command ATTN: AMCRD, Dr.J.V.R.Kaufman 5001 Eisenhower Avenue Alexandria, Virginia 22304
1	Commander U.S. Army Materiel Command ATTN: AMCRD-TE 5001 Eisenhower Avenue Alexandria, Virginia 22304
1	Commander U.S. Army Materiel Command ATTN: AMCRD-TP 5001 Eisenhower Avenue Alexandria, Virginia 22304
1	Commander U.S. Army Materiel Command ATTN: AMCRD-MT 5001 Eisenhower Avenue Alexandria, Virginia 22304
1	Commander U.S. Army Aviation Systems Command ATTN: AMSAV-E 12th and Spruce Streets St. Louis, Missouri 63166
1	Director U.S. Army Air Mobility Research and Development Laboratory Ames Research Center Moffett Field, California 94035
1	Commander U.S. Army Electronics Command ATTN: AMSEL-RD Fort Monmouth, New Jersey 07703
3	Commander U.S. Army Missile Command ATTN: AMSMI-R Mr. F. James Mr. N. White AMSMI-RK Redstone Arsenal, Alabama 35809
1	Commander U.S. Army Tank Automotive Command ATTN: AMSTA-RHFL Warren, Michigan 48090

DISTRIBUTION LIST

No. of Copies	Organization
2	Commander U.S. Army Mobility Equipment Research & Development Center ATTN: Tech Docu Cen, Bldg. 315 AMSME-RZT Fort Belvoir, Virginia 22060
1	Commander U.S. Army Munitions Command ATTN: AMSMU-RE Dover, New Jersey 07801
1	Commander U.S. Army Frankford Arsenal ATTN: SMUFA-L1000 Philadelphia, Pennsylvania 19137
1	Commander U.S. Army Picatinny Arsenal ATTN: SMUPA-VG Dover, New Jersey 07801
1	Commander U.S. Army White Sands Missile Range ATTN: STEWS-VT New Mexico 88002
2	Commander U.S. Army Weapons Command ATTN: AMSWE-RE AMSWE-RDF Rock Island, Illinois 61202
1	Director U.S. Army Advanced Materiel Concepts Agency 2461 Eisenhower Avenue Alexandria, Virginia 22314
1	Commander U.S. Army Harry Diamond Laboratories ATTN: AMXDO-TD/002 Washington, DC 20438
1	Commander U.S. Army Materials and Mechanics Research Center ATTN: AMXMR-ATL Watertown, Massachusetts 02172
1	Commander U.S. Army Natick Laboratories ATTN: AMXRE, Dr. D. Sieling Natick, Massachusetts 01762
2	Commander U.S. Army Research Office (Durham) ATTN: Mr. R. Heaston Tech Lib Box CM, Duke Station Durham, North Carolina 27706
5	Commander U.S. Naval Air Systems Command ATTN: AIR-5366 AIR-5367 AIR-604 (3 cys) Washington, DC 20360
3	Commander U.S. Naval Ordnance Systems Command ATTN: ORD-0632 ORD-035 ORD-5524 Washington, DC 20360
1	Chief of Naval Research ATTN: ONR-429 Department of the Navy Washington, DC 20360
1	Commander U.S. Naval Missile Center ATTN: Code 5632 Point Magu, California 93041

DISTRIBUTION LIST

No. of Copies	Organization
3	Commander U.S. Naval Weapons Center ATTN: Code 608 Mr. E. Price Mr. J. Crump Code 753, Tech Lib China Lake, California 93555
1	Commander U.S. Naval Ordnance Laboratory ATTN: Code 730 Silver Spring, Maryland 20910
1	Director U.S. Naval Research Laboratory ATTN: Code 6180 Washington, DC 20390
1	Commander U.S. Naval Weapons Laboratory ATTN: Tech Lib Dahlgren, Virginia 22338
1	Superintendent U.S. Naval Postgraduate School ATTN: Tech Lib Monterey, California 93940
2	Commander U.S. Naval Ordnance Station ATTN: Mr. L. Dickinson Tech Lib Indian Head, Maryland 20630
1	AFSC (DOL) Andrews AFB Washington, DC 20331
1	AFOSR (SREP) 1400 Wilson Boulevard Arlington, Virginia 22209
2	AFRPL (RPMCP; Tech Lib) Edwards AFB California 93523

No. of Copies	Organization
1	Director U.S. Bureau of Mines ATTN: ERC 4800 Forbes Street Pittsburgh, Pennsylvania 15213
2	Headquarters National Aeronautics and Space Administration ATTN: RPS RP Washington, DC 20546
1	Director NASA Scientific and Technical Information Facility ATTN: CRT P. O. Box 33 College Park, Maryland 20740
1	Director National Aeronautics and Space Administration George C. Marshall Space Flight Center ATTN: Tech Lib Huntsville, Alabama 35812
2	Director Jet Propulsion Laboratory ATTN: Mr. J. Strand Tech Lib 4800 Oak Grove Drive Pasadena, California 91103
1	Director John F. Kennedy Space Center, NASA ATTN: Tech Lib Kennedy Space Center Florida 32899

DISTRIBUTION LIST

No. of Copies	Organization
1	Director National Aeronautics and Space Administration Langley Research Center ATTN: MS-185, Tech Lib Langley Station Hampton, Virginia 23365
2	Director National Aeronautics and Space Administration Lewis Research Center ATTN: MS-603, Tech Lib MS-86, Dr. L. Povinelli 21000 Brookpark Road Cleveland, Ohio 44135
1	Director National Aeronautics and Space Administration Manned Spacecraft Center ATTN: Tech Lib Houston, Texas 77058
1	Aerojet Solid Propulsion Co. ATTN: Mr. P. L. Micheli Sacramento, California 95813
1	Aerospace Corporation ATTN: Tech Lib P. O. Box 95085 Los Angeles, California 90045
1	ARO Incorporated ATTN: Mr. N. Dougherty Arnold AFS, Tennessee 37389
1	Atlantic Research Corporation ATTN: Tech Lib Shirley Highway at Edsall Rd Alexandria, Virginia 22314
1	General Electric Company Flight Propulsion Division ATTN: Tech Lib Cincinnati, Ohio 45215
2	Hercules Powder Company Allegany Ballistic Laboratories ATTN: Mr. T. Angelus Tech Lib Cumberland, Maryland 21501
1	Hercules Powder Company Bacchus Division ATTN: Mr. M. Beckstead Magna, Utah 84044
2	Lockheed Propulsion Company ATTN: Dr. N. Cohen Mr. R. Derr P. O. Box 111 Redlands, California 92373
1	McDonnell Douglas Corporation Missile and Space Systems Division ATTN: Tech Lib Santa Monica, California 90406
1	The Marquardt Corporation ATTN: Tech Lib 16555 Saticoy Street Van Nuys, California 91404
1	The Martin-Marietta Corporation Denver Division ATTN: Res Lib P. O. Box 179 Denver, Colorado 80201
2	North American Rockwell Corp Rocketdyne Division ATTN: Mr. C. Oberg Tech Lib 6633 Canoga Avenue Canoga Park, California 91304

DISTRIBUTION LIST

No. of Copies	Organization
2	North American Rockwell Corp Rocketdyne Division ATTN: Mr. W. G. Haymes Tech Lib McGregor, Texas 76657
1	Northern Research and Engineering Corporation ATTN: Mr. K. Bastress Cambridge, Massachusetts 02179
1	Rocket Research Corporation ATTN: Tech Lib Seattle, Washington 98198
1	Thiokol Chemical Corporation Elkton Division ATTN: Tech Lib Elkton, Maryland 21921
2	Thiokol Chemical Corporation Huntsville Division ATTN: Mr. D. Flanigan Tech Lib Huntsville, Alabama 35807
1	Thiokol Chemical Corporation Wasatch Division ATTN: Tech Lib P. O. Box 524 Brigham City, Utah 84302
1	TRW Systems Group ATTN: Mr. H. Korman One Space Park Redondo Beach, California 90278
1	United Aircraft Corporation Pratt and Whitney Division ATTN: Tech Lib P. O. Box 2691 West Palm Beach, Florida 33402
1	United Aircraft Corporation Research Laboratories ATTN: Mr. R. Waesche East Hartford, Connecticut 06108
2	United Technology Center ATTN: Dr. R. Brown Tech Lib P. O. Box 358 Sunnyvale, California 94088
1	Battelle Memorial Institute ATTN: Tech Lib 505 King Avenue Columbus, Ohio 43201
2	Brigham Young University Dept of Chemical Engineering ATTN: Mr. R. Coates Dr. M. Horton Provo, Utah 84601
2	California Institute of Technology ATTN: Prof. F. Culick Tech Lib 1201 East California Boulevard Pasadena, California 91102
1	Calspan Corporation ATTN: Dr. G. Markstein P. O. Box 235 Buffalo, New York 14221
2	Georgia Institute of Technology School of Aerospace Engineering ATTN: Mr. B. Zinn Mr. W. Strahle Atlanta, Georgia 30333
1	IIT Research Institute ATTN: Mr. T. Torda 10 West 35th Street Chicago, Illinois 60616

DISTRIBUTION LIST

No. of Copies	Organization
1	Director Applied Physics Laboratory The Johns Hopkins University ATTN: Dr. R. Cantrell 8621 Georgia Avenue Silver Spring, Maryland 20910
2	Director Chemical Propulsion Information Agency The Johns Hopkins University ATTN: T. W. Christian Tech Lib 8621 Georgia Avenue Silver Spring, Maryland 20910
1	Pennsylvania State University Dept of Mechanical Engineering ATTN: Mr. G. Faeth University Park, Pennsylvania 16802
3	Princeton University Dept of Aerospace and Mechanical Sciences ATTN: Dr. M. Summerfield Dr. I. Glassman Tech Lib James Forrestal Campus Princeton, New Jersey 08540
1	Purdue University School of Mechanical Eng. ATTN: Dr. J. Osborn Lafayette, Indiana 47907
1	Rutgers-State University Dept of Mechanical and Aerospace Engineering ATTN: Dr. S. Temkin University Heights Campus New Brunswick, New Jersey 08901
1	Stanford Research Institute Propulsion Sciences Division ATTN: Tech Lib 333 Ravenswood Avenue Menlo Park, California 94025
1	Stevens Institute of Technology Davidson Laboratory ATTN: Dr. R. McAlevy III Hoboken, New Jersey 07030
2	University of California Dept of Aerospace Engineering ATTN: Dr. S. Penner Dr. F. Williams La Jolla, California 92037
1	University of California Department of Chemistry ATTN: Dr. E. Peterson Berkeley, California 94704
1	University of Denver Denver Research Institute ATTN: Tech Lib P. O. Box 10127 Denver, Colorado 80210
2	University of Illinois Dept of Aeronautical Eng ATTN: Prof. H. Krier Prof. R. Strehlow Urbana, Illinois 61803
1	University of Minnesota Dept of Mechanical Engineering ATTN: Dr. E. Fletcher Minneapolis, Minnesota 55455
2	University of Utah Dept of Chemical Engineering ATTN: Mr. A. Baer Mr. G. Flandro Salt Lake City, Utah 84112

DISTRIBUTION LIST

Aberdeen Proving Ground

Chief, Tech Lib
Marine Corps Ln Ofc
CDC Ln Ofc
Dir, USAMSAA
ATTN: Dr. J. Sperrazza

UNCLASSIFIED

Security Classification

DOCUMENT CONTROL DATA - R & D

(Security classification of title, body of abstract and indexing annotation must be entered when the overall report is classified)

1. ORIGINATING ACTIVITY (Corporate author) Interior Ballistics Laboratory Ballistic Research Laboratories Aberdeen Proving Ground, Md. 21005	2a. REPORT SECURITY CLASSIFICATION Unclassified 2b. GROUP

3. REPORT TITLE

Effects of a Magnetic Field on Burning Rate of Solid Propellant

4. DESCRIPTIVE NOTES (Type of report and inclusive dates)

5. AUTHOR(S) (First name, middle initial, last name)

Webster M. Kendrick, Leland A. Watermeier,
William P. Aungst, Samuel P. Pfaff

6. REPORT DATE	7a. TOTAL NO. OF PAGES	7b. NO. OF REFS
June 1973	39	2

8a. CONTRACT OR GRANT NO.	9a. ORIGINATOR'S REPORT NUMBER(S)
b. PROJECT NO. 1T161102A33C	BRL Report No. 1650
c.	9b. OTHER REPORT NO(S) (Any other numbers that may be assigned this report)
d.	

10. DISTRIBUTION STATEMENT

Approved for public release; distribution unlimited.

11. SUPPLEMENTARY NOTES	12. SPONSORING MILITARY ACTIVITY
	U. S. Army Ballistic Research Labs Aberdeen Proving Ground, Md. 21005

13. ABSTRACT

Preliminary experiments conducted by the Interior Ballistics Laboratory to determine if a magnetic field applied during low pressure combustion of solid propellant can alter the burning rate have shown positive results. Experiments were conducted with a field strength of 15000 gauss applied to composite propellants containing aluminum additive burning at atmospheric and sub-atmospheric pressures. Although results showed wide scatter of data, it appears that burning rate variations of ± 10% could be obtained.

DD FORM 1 NOV 68 1473 REPLACES DD FORM 1473, 1 JAN 64, WHICH IS OBSOLETE FOR ARMY USE.

UNCLASSIFIED

Security Classification

14. KEY WORDS	LINK A		LINK B		LINK C	
	ROLE	WT	ROLE	WT	ROLE	WT
Solid propellants Magnetic field effects on combustion Low pressure propellant combustion Combustion Composite propellant burning Ambipolar diffusion in magnetic field						